Review Article

BIOMEDICAL Journal of Scientific & Technical Research

ISSN: 2574 -1241

DOI: 10.26717/BJSTR.2019.18.003106

A. Appendix

Relevant equations

Table A.1: Equations to calculate IDR and TADR. Unless stated otherwise, all equations were taken from [1].

1. Barrier transmission factor	(5)
2. Number of TVLs	(6)
3. Thickness of a material	(7)
4. IDR behind a primary barrier	(8)
5. TADR behind a primary barrier	(9)
6. IDR behind a secondary barrier	(10)
7. TADR behind a secondary barrier	(11)
8. IDR at maze entrance due to beam scatter off of bunker wall when beam is parallel to maze entrance	(12)
9. IDR at maze entrance due to beam scatter off the bunker wall when beam is perpendicular to maze entrance	$IDR_2 = \prod_{n=1}^{n=n} \frac{B \times S^* \times \alpha_{n_{wall}} \times A_{n_{wall}} \times 60}{(d_{i_{wall}} \times d_{n_{wall}})^2}$ (13)
10. TADR at maze entrance due to beam scatter off the bunker wall when beam is parallel to maze entrance	$TADR_1 = \prod_{n=1}^{n=n} \frac{D_f \times N \times 250 \times U \times T \times \alpha_{n_{wall}} \times A_{n_{wall}}}{(d_{i_{wall}} \times d_{n_{wall}})^2}$ (14)
11. TADR at maze entrance due to beam scatter off the bunker wall when beam is perpendicular to maze entrance	$TADR_1 = \prod_{n=1}^{n=n} \frac{B \times D_f \times N \times 250 \times U \times T \times \alpha_{n_{wall}} \times A_{n_{wall}}}{(d_{i_{wall}} \times d_{n_{wall}})^2}$ (15)
12. IDR due to scatter off patient	$IDR_2 = \prod_{n=1}^{n=n} \frac{S^* \times \alpha \times \alpha_{n-1_{pat}} \times A_{n-1_{pat}} \times 60 \times \frac{F}{400}}{(d_{i_{pat}} \times d_{n_{pat}})^2}$ (16)
13. TADR due to scatter off the patient	$TADR_2 = \prod_{n=1}^{n=n} \frac{D_f \times \alpha \times \alpha_{n-1_{pat}} \times A_{n-1_{pat}} \times 250 \times N \times \frac{F}{400} \times T}{(d_{i_{pat}} \times d_{n_{pat}})^2}$ (17)
14. IDR due to head leakage scatter	$IDR_3 = \prod_{n=1}^{n=n} \frac{S^* \times 0.001 \times \alpha_{n-1_{HL}} \times A_{n-1_{HL}} \times 60}{(d_{i_{HL}} \times d_{n_{HL}})^2}$ (18)
15. TADR due to head leakage scatter	$TADR_3 = \prod_{n=1}^{n=n} \frac{D_f \times 250 \times N \times f \times 0.001 \times \alpha_{n-1_{HL}} \times A_{n-1_{HL}} \times T}{(d_{i_{HL}} \times d_{n_{HL}})^2}$ (19)
16.IDR due to head leakage transmission	$IDR_4 = S^* \times 0.001 \times \frac{B_{Co-60}}{(d_m)^2}$ (20)
17. TADR due to head leakage transmission	$TADR_4 = D_f \times N \times 250 \times f \times 0.001 \times T \times \frac{B_{Co-60}}{(d_m)^2}$ (21)

Table A.2: Equations associated with neutron production [1].

1. Neutron fluence at point A in appendix Figure K.1	[16] $\phi_A = \frac{\beta Q}{4\pi d^2_{1_n eut}} + \frac{5.4\beta Q}{2\pi S} + \frac{1.3Q}{2\pi S}$ (22)
2. The IDR dose equivalent at the maze entrance of the neutron capture gamma rays	[18] $H_{\gamma IDR} = S^* \times 60 \times 6.9 \times 10^{16} \times \phi_A \times 10^{-\frac{d_2}{TVD_{1neutron}}}$ (23)
3. The TADR dose equivalent at the maze entrance of the neutron capture gamma rays	[18] $H_{\gamma TADR} = D_f \times N \times 250 \times f \times T \times 6.9 \times 10^{16} \times \phi_A \times 10^{-\frac{d_2}{TVD_{1neutron}}}$ (24)
4. Neutron dose equivalent at the maze entrance	[19] $H_n = \frac{2.4 \times 10^{-15} \times \phi_A \times (\frac{S_0}{S_1})^{0.5} \times (1.64 \times 10^{\frac{-d_2}{1.9}} + 10^{\frac{-d_2}{TVD_2}})}{3^{n-2}}$ (25)
5. Tenth value distance2	[1] $TVD_2 = 2.06 \times (S_1)^{0.5}$ (26)
6. Transmission barrier of door at end of maze	[1] $B = DR_{acc} / DR_i$ (27)

B. Explanations of Symbols Used

1. TVL_1 and TVL_e	First tenth value layer and equilibrium tenth value layer
2. IDR	Instantaneous dose rate
3. $TADR$	Time annual dose rate
4. DR_i	Dose rate at the isocenter
5. d_i	Distance to isocenter
6. d_p	Distance from target to 0.3m from barrier, on the other side of barrier
7. f	Fractional increase in 'beam-on time'
8. U	Orientation factor (fraction of time beam is pointed in a certain direction)
9. T	Occupancy factor (fraction of time the area is occupied by an individual)
10. S^*	Dose rate at the isocenter
11. $\alpha_{n_{wall}}$	The reflection coefficient at the maze wall
12. $A_{1_{wall}}{}^*$	The beam area at the first scatter
13. F_L	the length of the field size incident on the patient.
14. $A_{n_{wall}}{}^*$	Area of the maze wall from which scatter is able to travel down the maze after the nth scatter off the wall.
15. $d_{i_{wall}}{}^*$	Distance from the target to primary barrier
16. $d_{n_{wall}}$	Distance from the nth scatter to the next maze entrance
17. D_f	Average dose per patient
18. N	Number of patients per day
19. α	Patient scatter factor
20. $\alpha_{n-1_{pat}}$	Reflection coefficient of the nth scatter from the maze wall due to patient scatter

21. $A_{n-1_{pat}}$ *	Area of the maze wall from which scatter is able to travel down the maze after the nth scatter off the wall due to patient scatter.
22. F	Field size incident on patient
23. $d_{i_{pat}}$ *	Distance from the target to the isocenter
24. $d_{n_{pat}}$ *	Distance from the nth patient scatter to the next maze entrance
25. $\alpha_{n-1_{HL}}$	Reflection co-efficient of the nth scatter from the maze wall due to head leakage scatter
26. $A_{n-1_{HL}}$ *	Area of the maze wall from which scatter is able to travel down the maze after the nth scatter off the wall due to head leakage scatter.
27. $d_{i_{HL}}$ *	Distance from the target to the isocenter
28. $d_{n_{HL}}$ *	Distance from the nth head leakage scatter to the next maze entrance
29. d_m *	Shortest distance through wall(s) from target to maze entrance
30. n	Number of legs
31. β	Head shielding transmission factor for neutrons (1 for lead, 0.85 for tungsten)
32. Q	Neutron source strength per gray
33. $d_{1_{neut}}$ *	Distance from isocenter to point A in appendix Figure K.1
34. S	Surface area of room
35. TVD_1	5.4m for x-rays in the range 18-25MV and 3.9m otherwise [14]
36. $d_{2_{neut}}$	Distance from point A to the outer maze entrance, following the maze
37. S_0 and S_1	Cross sectional area of inner maze entrance and cross-sectional area of maze respectively
38. B_M	Cobalt-60 Transmission coefficient of inner maze wall (Use Co-60 TVL values to find NM)
39. B_r	Required transmission factor
40. B_c	Calculated transmission factor
41. n_r	Required number of TVLs
42. n_c	Calculated number of TVLs
43. EA, EB and EC	Energy of beam A, B and C respectively
44. $frac_A$, $frac_B$ and $frac_c$	fraction of treatments completed at beam A, B and C respectively

* - Appendix Figures I.1 & I.2 show how the values of A_{ni} and d_{ni} were found (where n is the respective scatter number and i can be the wall, patient or Head scatter leakage (Note, the coefficients for $A_{npatient}$ and A_{nhead} leakage are equal. The same applies to finding the values of $d_{npatient}$ and d_{nhead} leakage).

Table B.1: Explanations of symbols used [1].

C. User Entered Parameters to Each Program

C.1. Primary Barrier IDR

The following parameters are inputted by the user into the primary barrier IDR program:

1. Material to be used as barrier
2. Energy of beam used
3. Thickness of barrier
4. Dose rate at the isocenter
5. Distance from isocenter to distance 0.3m from barrier on other side of barrier
6. Treatment head to isocenter distance

C.2. Secondary Barrier IDR

The following parameters are inputted by the user into the secondary barrier IDR program:

1. Material to be used as barrier
2. Energy of beam used
3. Thickness of barrier
4. Dose rate at the isocenter
5. Distance from isocenter to distance 0.3m from barrier on other side of barrier

C.3. Primary Barrier TADR

The following parameters are inputted by the user into the primary barrier TADR program:

1. Material to be used as barrier
2. Energy of up to three beams used throughout a year. These energies are:

a) Energy A (EA), Energy B (EB) and Energy C (EC), the energies of beams A, B and C respectively.

3. The fraction of treatments each beam is used for:

a) *fracA, fracB* and *fracC*, the fraction of treatments completed using energy beam A, B and C respectively.

4. Thickness of barrier
5. Dose rate at the isocenter
6. Distance from isocenter to distance 0.3m from barrier on other side of barrier
7. Treatment head to isocenter distance

C.4. Secondary Barrier TADR

The following parameters are inputted by the user into the secondary barrier TADR program.

1. Material to be used as barrier

2. Energy of up to three beams used throughout a year. These energies are:

a) Energy A (EA), Energy B (EB) and Energy C (EC), the energies of beams A, B and C respectively.

3. The fraction of treatments each beam is used for:

b) *fracA, fracB* and *fracC*, the fraction of treatments completed using energy beam A, B and C respectively.

4. Thickness of barrier

5. Dose rate at the isocenter

6. Distance from isocenter to distance 0.3m from barrier on other side of barrier

C.5. Maze Scatter

The parameters the user is asked to enter are summarized in Table C.1.

Variable	Symbol
1. Material of maze	*material*
2. Orientation of beam with respect to maze	*Orientation*
3. Distance from isocenter to maze entrance	d_m
4. Room width	RW
5. Room height	RH
6. Room length	RL
7. Effective energy of beam after first scatter	Eff_E
8. Maze height	MH
9. Number of legs in maze	$leg_{no.}$
10. Width of inner maze entrance	$S_{0_{width}}$
11. Width of maze	$S_{1_{width}}$
12. Material of target	*Target*
13. Width of areas exposed by radiation *	$A_{2_{wall_w}}, A_{3_{wall_w}}, A_{4_{wall_w}}, A_{1_{pat_w}}, A_{2_{pat_w}}, A_{3_{pat_w}}, A_{1_{HL_w}}, A_{2_{HL_w}}, A_{3_{HL_w}}$
14. Value of d1 etc.*	$d_{1_{wall}}, d_{2_{wall}}, d_{3_{wall}}, d_{4_{wall}}, d_{1_{pat}}, d_{2_{pat}}, d_{3_{pat}}, d_{1_{HL}}, d_{2_{HL}}, d_{3_{HL}}$
15. Angles of incidence and reflection of wall, patient and head leakage respectively	$\theta_{i_w}, \theta_{r_w}, \theta_{i_p}, \theta_{r_p}, \theta_{i_{HL}}, \theta_{r_{HL}}$
16. Energy A, B and C	EA, EB and EC
17. Percentage of treatments each beam is used	$frac_A, frac_B$ and $frac_c$

18. Average dose per patient	D_f
19. Orientation factor	U
20. Occupancy factor	T
21. Number of patients per day	N
22. IMRT factor	$IMRT_{factor}$
23. IMRT fraction	$IMRT_{fraction}$
24. Annual dose constraint	$TADR_{constraint}$
25. Neutron production per gray for each energy beam	Q_A, Q_B and Q_c

* means if required.

As it is assumed three separate energy beams are used throughout the year, individual values for every energy-dependent variable must be found for each energy beam, taking into account the percentage of treatments this beam is used for.

C.6. Cyber Knife - Direct Door

The following parameters are inputted by the user into the Cyber knife - Direct door algorithm:

1. Treatment head to isocenter distance

2. Distance from barrier to point 0.3m on from barrier on other side of barrier

3. Dose rate at isocenter

4. IDR constraint

5. Average dose per patient

6. Orientation factor

7. Number of patients per day

8. Occupancy factor

9. IMRT factor

10. IMRT fraction

11. TADR constraint

D. Working Principles of linac

D.1. Working Principles of Linac

After leaving the waveguide, the beam enters the Flight Tube, as shown in Figure D.1. Here three magnets bend and focus the beam such that it hits it's intended target, whilst also narrowing the beam, giving it a diameter of approximately 1mm. The design of the magnets allows them to focus electrons of different energies onto the same point on the target, which is known as aromatic behaviour.

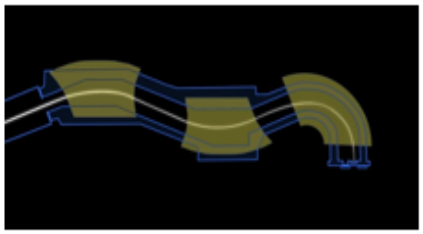

Figure D.1: Flight Tube [17].

Figure D.2: Primary Collimator [17].

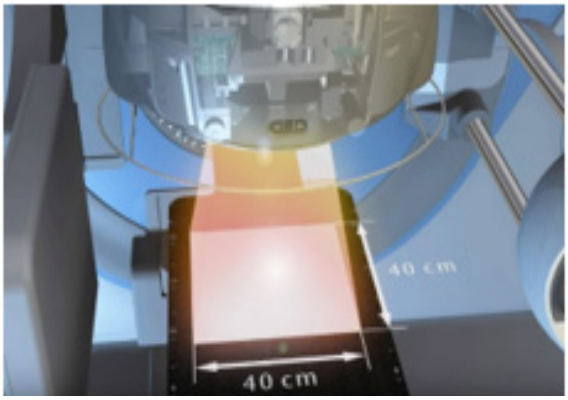

Figure D.3: Collimators are also defining the maximum field size of the resulting clinical radiation beam [17].

Once the electron beam hits the target, the electron's energy is converted into x-rays. High energy photons emerge from the target in all directions and require head shielding to attenuate this leakage radiation. However, the primary collimator situated under the target allows rays travelling in forward direction to pass through. This is the beam that is used to treat the patient

with field sizes varying from 2x2cm to 40x40cm. This defines the maximum field size of 40cm by 40cm at the isocenter. An advantage of the collimator is to minimize leakage by absorbing scattered x-rays travelling in the lateral direction. As seen in figure D.4, the photon beam is non-uniformly distributed when it emerges from the target. Hence a Flattening Filter, as seen in Figure D.5 is used to give a uniform beam distribution.

D.2. Monitor Unit Delivery

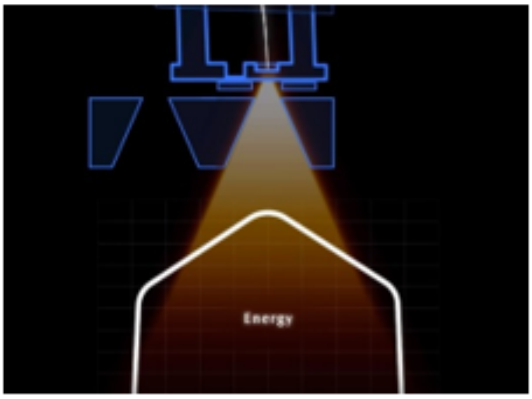

Figure D.4: Non-uniform photon distribution [17].

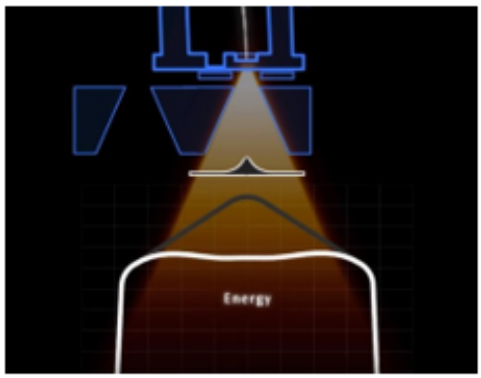

Figure D.5: Uniform photon beam distribution due to introduction of flattening filter [17].

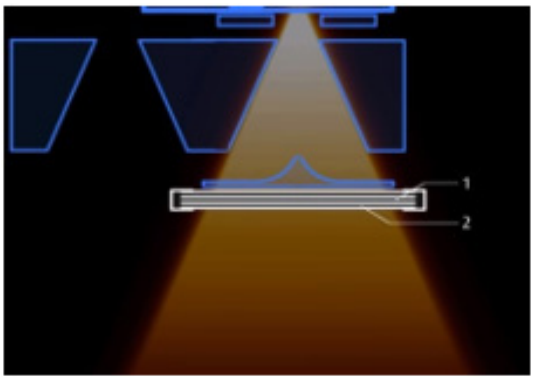

Figure D.6: Ion chamber to measure radiation dose [17].

Two simultaneous ion chambers located in the beam (illustrated in figure D.6) are used to measure the dose and beam quality monitoring. One is the primary dosimeter and terminates the radiation when the required dose has been delivered, whilst the second chamber acts as a backup, and stops the radiation if the primary chamber fails. Due to the electrical nature of beam production, the linac output fluctuates. The ion chambers measure the amount of radiation that travels through them (taking account of fluctuations and terminates when a pre-determined amount of radiation has been reached). This measurement is called Monitor Units (MUs) and generally 1cGy=1MU for a 10 10 field size at the isocenter. The treatment beam must replicate the beam modelled within the planning system. A beam quality function is performed by a third ionization chamber, which uses seven electrodes to monitor different sections of the radiation field.

E. Other Treatment Modalities

E.1. Conformal Radiotherapy

Conformal radiotherapy is the most common form of radiotherapy treatment in Ireland. Collimators are used to confine the radiation to the defined area. Multileaf collimators (MLC) can be used to produce irregularly shaped fields in order to mimic the shape of irregularly shaped tumors, thus allowing the radiation to strike the tumor and evode organs at risk (OAR) or healthy tissue. The MLC consists of a number of sheets of high-density metal, known as leaves, that absorb the radiation. These leaves cast a radiation shadow at the isocenter [1].

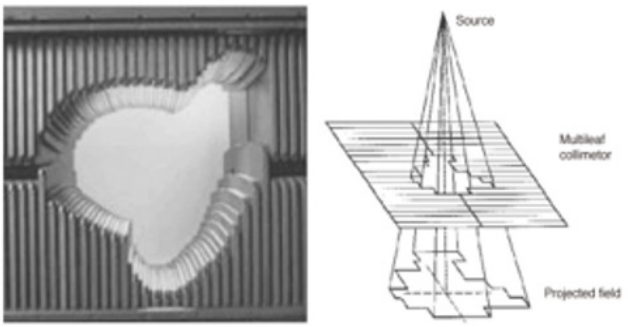

Figure E.1: Conformal Therapy can be used by the application of multileaf collimators (MLC) to a traditional linear accelerator [18].

E.2. Intensity Modulated Radiotherapy (IMRT)

By changing the field shape of the MLC during treatment, it is possible to give different doses to different parts of the tumor. This is becoming an increasingly more popular treatment in radiotherapy departments as it allows the planner to 'bend radiation' and develop more complex shapes that were not possible using conformal radiotherapy. It does this by creating fields within fields to vary the intensity of the beam. It has the advantage of being able to deliver higher radiation doses to the tumor while saving the normal or healthy tissue. IMRT can be delivered via two methods - step and shoot, and dynamic. The downside of IMRT is that in either case, the beam on time (MUs) and hence leakage radiation is significantly greater (2-5 times) than conformal therapy. The target dose is directly proportional to the number of MUs. For step and shoot, each mini field is irradiated, the beam turned off and the leaves moved to the next mini field position, before turning on the beam once again. This process is repeated until complete. The number of MUs required compared to simple conformal treatment will be approximately 2.5 times greater for step and shoot IMRT. With the dynamic method, the leaves are moved continuously with the beam turned on, with the number of MUs required compared to conformal

treatment being approximately 5 times greater. This multiplying factor is referred to as the IMRT factor and calculations of the shielding required in secondary barriers need to include this factor to allow for the increased treatment time [1].

E.3. Volumetric Modulated Arc Therapy (Vmat)

This development of dynamic IMRT has been called VMAT. In this approach the gantry rotates continuously around the patient at a variable speed, the positions of the MLC leaves are continually adjusted, and the dose rate is varied. The greatly increased number of beam orientations facilitates the delivery of even more precisely conformed dose distributions than IMRT. The efficiency in terms of the number of MUs to give a specified dose to the patient is roughly equivalent to step-and-shoot, i.e. the IMRT factor is 2.5. In addition, the dose exiting from the patient is distributed more uniformly over the primary barrier leading to less radiation escaping the bunker in any given direction [1].

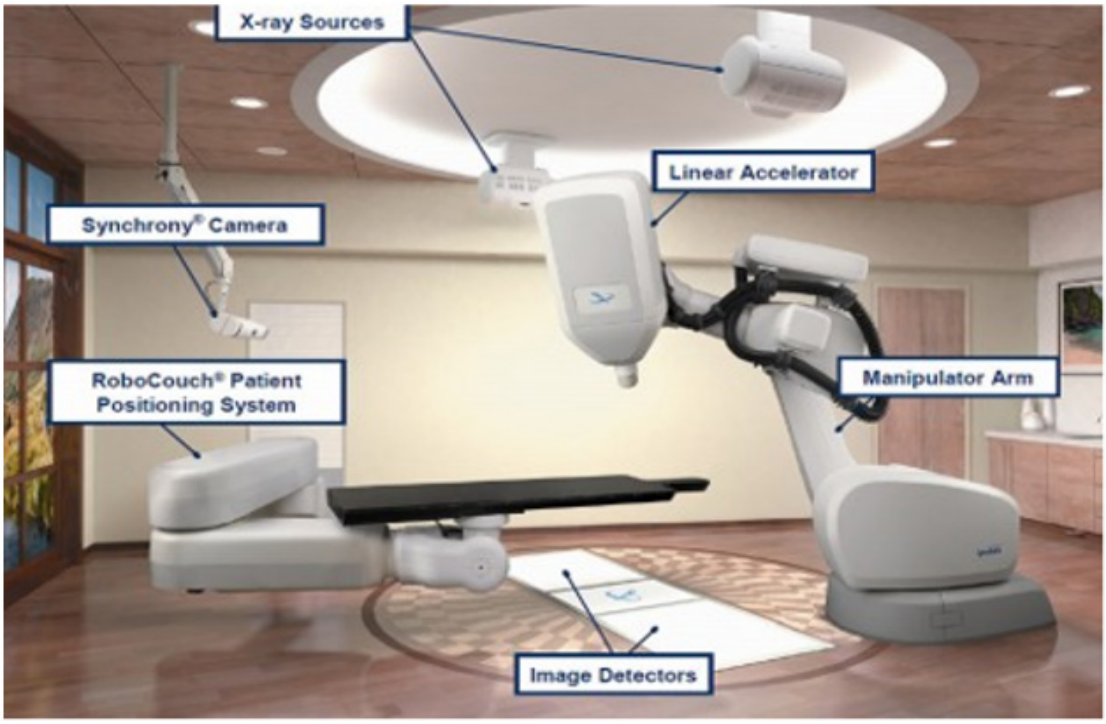

Figure E.2: Cyberknife Unit [19].

The Cyber Knife Unit (seen in Figure E.2, does not use isocentric design. A 6MV beam is mounted on a robotic arm which allows the beam to be pointed at any point within the patient under robotic control, with the restriction of not being pointed more than 18-22(◦) above the horizontal. As the beam can be pointed in any direction, with some restriction in the upward direction, all the walls become primary barriers. Although each wall will only be irradiated for a small portion of time. The center of treatment is defined by the center of the imaging system (termed 'the room imaging center'). The imaging system consists of two x-ray tubes mounted on the ceiling of the room together with two digital imaging plates located in the floor. Most treatments are given using only 1–5 fractions with 5–30 Gy per fraction. This means that the number of monitor units is very high for each fraction, but the number of patient treatments per day is much less than a conventional linear accelerator [1].

E.5. Flattening Filter Free (FFF)

Flattening filter is used to make a uniform beam. The filter increases the penetrative quality of the beam in the centre of the field and produces the desired uniform dose across the beam whilst reducing the beam intensity on the central axis [1]. When using stereotactic treatments, the mini fields are small and the need for a flat uniform dose distribution across a field is much reduced. Therefore, the flattening filter is not necessary and can be removed to produce FFF beams. Because the heavy metal filter is removed, FFF beams have a higher dose than with a filter. The absence of a flattening filter also removes the major contributor to the magnitude of head leakage radiation by approximately 50% [1].

F. Calculating TADR Variables Dependent on Different Energies

As the values such as TVL, α (patient scatter factor) and αn (including αnwall and αn-1patient) are dependent on the energy of the beam used and it is assumed that three energy beams are used throughout a year, the algorithm must be modified using the method found below to accurately reflect the different use factors of each beam.

F.1. Method for Calculating TADR Variables Dependent on Different Energies

The example below illustrates how to accurately find the value of α1wall during a period when different energy beams are used. This method is not restricted to α1wall and is used to find all reflection coefficients associated with scatter, along with values such as n, TVL, TADR, tincrease, φA, HγTADR.

1. α1wall is found (the reflection coefficient due to EA) as described in section (2.8.5)

2. This value must be multiplied by the fraction of treatments EA is used for within a year to get α1wallA (α1wallA = α1wallA1× fracA), the absolute value of the reflection coefficient.

3. This process is repeated for EB and EC (obtaining α1wall and α1wall respectively).

4. The total value of α1wall can be found by summing the individual components together.

The method described above can be used to accurately calculate the value of energy- dependent variables for TADR equations where a number of different energy beams are used.

G. TVL values

Table G.1: Primary beam TVLs for concrete, steel and lead from a range of endpoint energies [14].

Energy	Concrete (m)		Steel (m)		Lead (m)	
MeV	TVL_1	TVL_e	TVL_1	TVL_e	TVL_1	TVL_e
4	0.35	0.3	0.099	0.099	0.057	0.057
6	0.37	0.33	0.1	0.1	0.057	0.057
10	0.41	0.37	0.11	0.11	0.057	0.057
15	0.44	0.41	0.11	0.11	0.057	0.057
18	0.45	0.43	0.11	0.11	0.057	0.057
20	0.46	0.44	0.11	0.11	0.057	0.057
25	0.49	0.46	0.11	0.11	0.057	0.057
30	0.51	0.49	0.11	0.11	0.057	0.057
Co-60	0.21	0.21	0.7	0.7	0.04	0.04

Table G.2: Leakage TVL values for concrete, steel and lead from a range of endpoint energies [14].

Energy	Concrete (m)		Steel (m)		Lead (m)	
MeV	TVL_1	TVL_e	TVL_1	TVL_e	TVL_1	TVL_e
4	0.33	0.28	0.099	0.099	0.057	0.057
6	0.34	0.29	0.1	0.1	0.057	0.057
10	0.35	0.31	0.11	0.11	0.057	0.057
15	0.36	0.33	0.11	0.11	0.057	0.057
18	0.36	0.34	0.11	0.11	0.057	0.057
20	0.36	0.34	0.11	0.11	0.057	0.057
25	0.37	0.35	0.11	0.11	0.057	0.057
30	0.37	0.35	0.11	0.11	0.057	0.057
Co-60	0.21	0.21	0.7	0.1	0.04	0.04

H. TADR neutron production and scatter

H.1. Scatter Factor Values

The relevant reflection coefficients needed for wall scatter (αnwall), patient scatter (αn-1pat), head leakage scatter (αn-1HL) (found in Tables H.1&H.2 and patient scatter factor (found in Table H.3) were automatically implemented into the algorithm through the use of the following spreadsheets after the relevant parameters are entered by the user. These parameters are:

1. The angle of incidence4(θi)
2. The angle of reflection4 (θr)
3. Energy of the beam
4. Material used in maze
5. Effective energy after the first scatter has occurred

Table H.1: Reflection coefficients for normal incidence on concrete as a function of angle of reflection for several endpoint energies [14].

Energy	Reflection coefficient 10^3 for normal incidence on concrete				
MeV	Angle of reflection ((°)) Measured from the normal				
Height	0	30	45	60	75
4	6.7	6.4	5.8	4.9	3.1
6	5.3	5.2	4.7	4	2.7
10	4.3	4.1	3.8	3.1	2.1
15	3.738	3.66	3.3	2.7	1.8
18	3.4	3.4	3	2.5	1.6
24	3.2	3.2	2.8	2.3	1.5
30	3	2.7	2.6	2.2	1.5
Co-60	7	6.5	6	5.5	3.8
Effective energy					
0.25	32	28	25	22	13
0.5	19	17	15	13	8

Table H.2: Reflection coefficients for 45o incidence on concrete as a function of angle of reflection for several endpoint energies [14].

Energy	Reflection coefficient 10^3 for 45° incidence on concrete				
MeV	Angle of reflection ((°)) Measured from the normal				
height	0	30	45	60	75
4	7.6	8.5	9	9.2	9.5
6	6.4	7.1	7.3	7.7	8
10	5.1	5.7	5.8	6	6
15	4.725	5.1	5.05	4.9	4.75
18	4.5	5.6	4.6	4.3	3.4
24	3.7	3.9	3.9	3.7	3
30	4.8	5	4.9	4	13
Co-60	9	10.2	11	11.5	12
Effective energy					
0.25	36	34.5	31	25	18
0.5	22	22.5	22	20	18

Table H.3: Scatter fractions at 1m from a human phantom for a reference field size of 400 cm^2 and target to phantom distance of 1 m [14].

Scatter fraction 10^3					
Angle (°)	**6 MV**	**10 MV**	**15 MV**	**18 MV**	**24 MV**
10	10.4	16.6	N/A	14.2	17.8
20	6.73	5.79	N/A	5.39	6.32
30	2.77	3.18	3.56	2.53	2.74
45	1.39	1.35	1.05	0.864	0.83
60	0.824	0.746	0.5	0.424	0.386
75	0.625	0.564	0.56	0.3065	0.28
90	0.426	0.381	N/A	0.189	0.174
135	0.3	5	N/A	0.124	0.12
150	0.287	274	N/A	0.12	0.113

I. Maze Scatter Workings

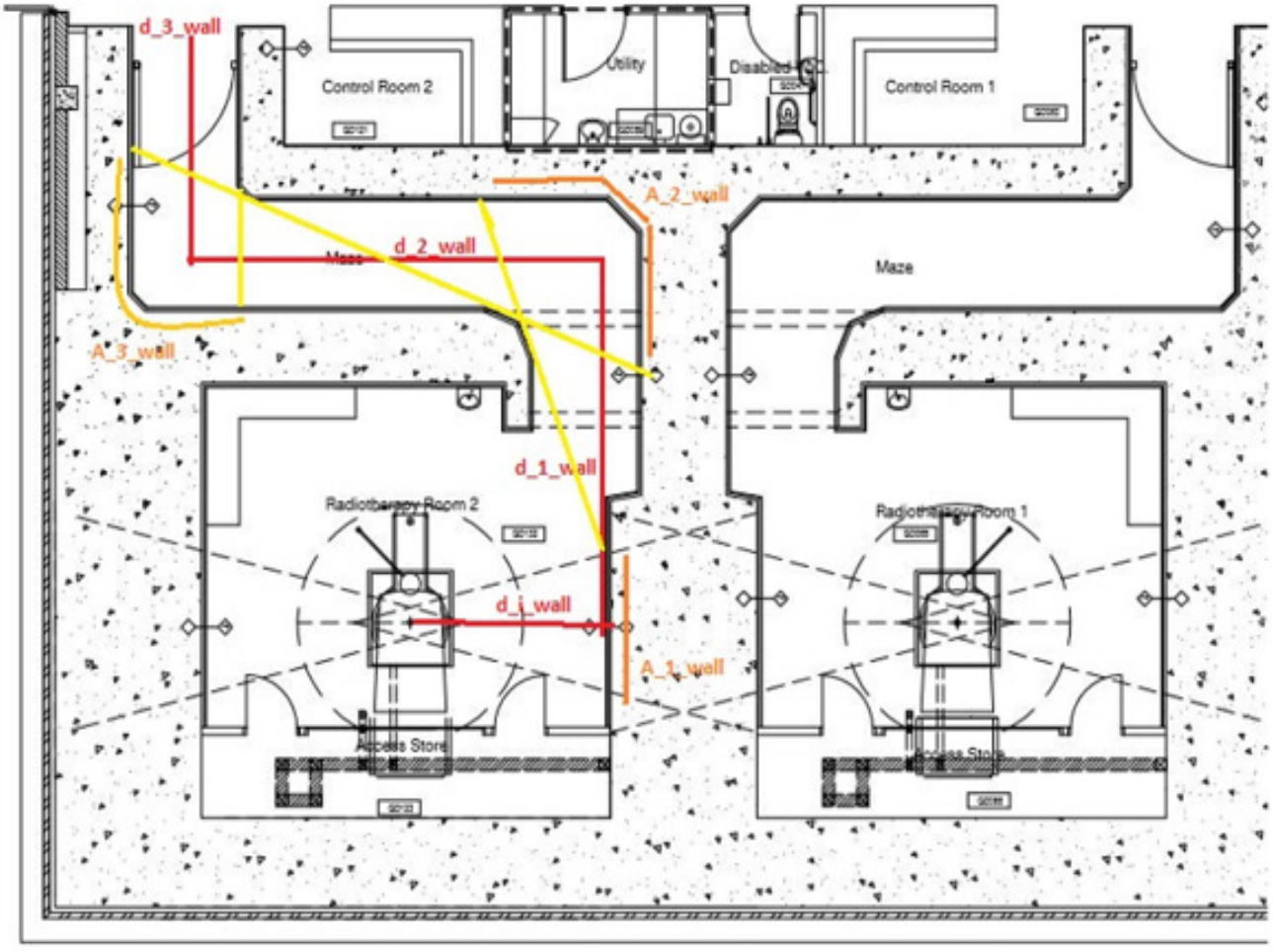

Figure I.1: Calculating Wall scatter contribution to maze scatter (Image is of The Hermitage Medical clinic radiotherapy bunker.

 DOI: 10.26717/BJSTR.2019.18.003106

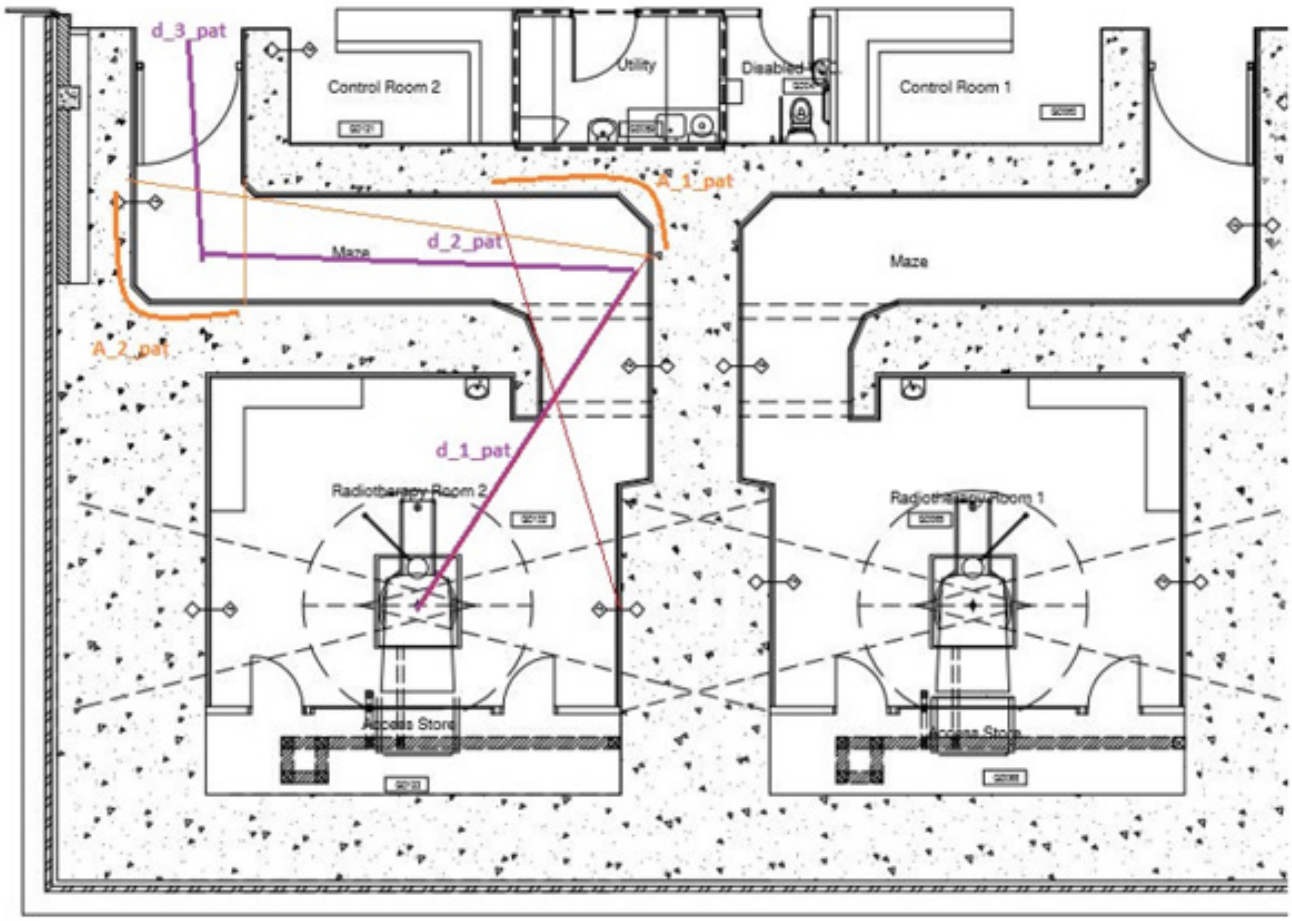

Figure I.2: Calculating patient scatter contribution to maze scatter Image is of *The Hermitage Medical clinic radiotherapy bunker*.

J. GUI (Graphical User-Interference)

J.1. Tkinter

To import Tkinter as a package to python, the following code was constructed

import Tkinter

from Tkinter import*

J.1.1. Top Level: In some instances, within the algorithm, a window is opened within a window, through use of Tkinter 's Top Level function. When Top Level is used, it creates a new window, independent of its parent window. This window is created within a local function; hence it does not affect the parent window. For this reason, it is only used for visualization purposes.

J.1.2. Text entry flowchart: The above figure is a sample of a value being inputted via a text box. The labelled numbers refer to the labelled numbers in the flowchart in figure 3.5. The sample used was that of inputting the IMRT factor (IF).

J.1.3. Drop Down Menu Selection: The above figure is a sample of a variable being selected from a drop-down selection menu. The labelled numbers in figure (J.2) refer to the labelled numbers in the flowchart in figure (3.6). The sample used was that of selecting the energy beam used for the IDR component of maze scatter.

```
1  IF=1
(1) 2  sIF = StringVar() #Command used to print answers in window
3  IF_test = StringVar()
(2) 4  IF_test.set('%s'  %IF)
(3) 5  IF_test_entry = Entry(root, width=6, textvariable=IF_test)
6  IF_test_entry.grid(row=8, column=1)
7
(4) 8  IF_label = Label(root, text='IMRT Factor', font="Calibri 10 bold")
9  IF_label.grid(row=8, column=0)
10
11 def comp_IF(event):
12     global sIF
13     global IF
14     global val_IF
15     val_IF = IF_test_entry.get()
16     try:
17         IF=float(val_IF)
18      (6) if IF >=0:
19          (7) sIF.set("IMRT factor = %g " %IF)
20         else:
21             sIF.set("Validate")
22         (8) IF_test_entry.delete(0, END) #deletes value if negative
23     except:
24         (8) sIF.set("Validate")
25             IF_test_entry.delete(0, END)   #deletes value if not a float
26
(5) 27 IF_test_entry.bind('<Return>', comp_IF) #Allows user to use return key as submit button
28
9) 29 IMRT_factor_label = Label(textvariable=sIF, width=25)
   IMRT_factor_label.grid(row=8, column=2)
```

Figure J.1: Code used to create text entry boxes for the IMRT factor.

```
1  s_enrg_IDR=StringVar()
2  E_IDR=StringVar(root_IDR)
3  E_IDR.set("Energy IDR")
4
(3) 5  def getE_IDR(*args):
6      s_enrg_IDR.set("{}MV was chosen".format(E_IDR.get()))
7
8  E_IDR.trace("w", getE_IDR)
9
10 #Energy drop down menu
(1) 11 drop_menu22=OptionMenu(root_IDR, E_IDR, "4", "6", "10", "15", "18", "20", "25", "30")
12 drop_menu22.grid(row=0, column=1)
13
(3) 14 energy_label_IDR=Label(textvariable=s_enrg_IDR, width=25)
15 energy_label_IDR.grid(row=0, column=2)
16
17
18 #Label energy
(2) 19 label_left_energy_IDR=Label(root_IDR, text="Select energy", font="Calibri 10 bold")
20 label_left_energy_IDR.grid(row=0, column=0)
```

Figure J.2: Code used to create drop down menu selection.

J.2. Executable

In order to set up the file as an executable, the following procedure was followed:

1. Save the following code as python file under the name setup.py, in the same folder as the desired file to be executed:

"from distutils. core import setup import py2exe

2. setup(console=['"Insert name of file to be executed here".py'])".

3. Once this is completed, the folder within which the setup.py is saved and must be opened in the Command prompt.

4. "setup.py py2exe"

was typed into command prompt the program can now be run as an executable on any computer.

K. Miscellaneous

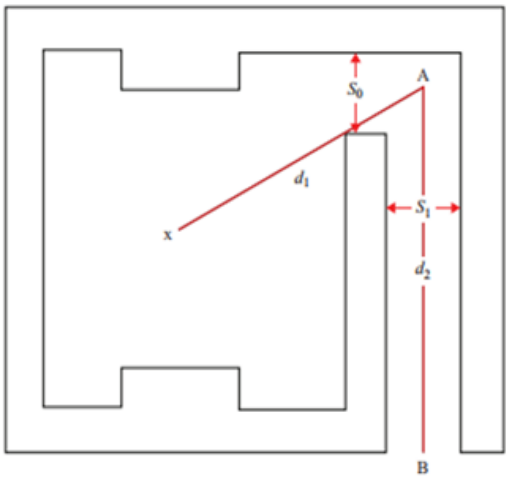

Figure K.1: Bunker plan showing the factors for calculation of the neutron fluence at the maze entrance [1].

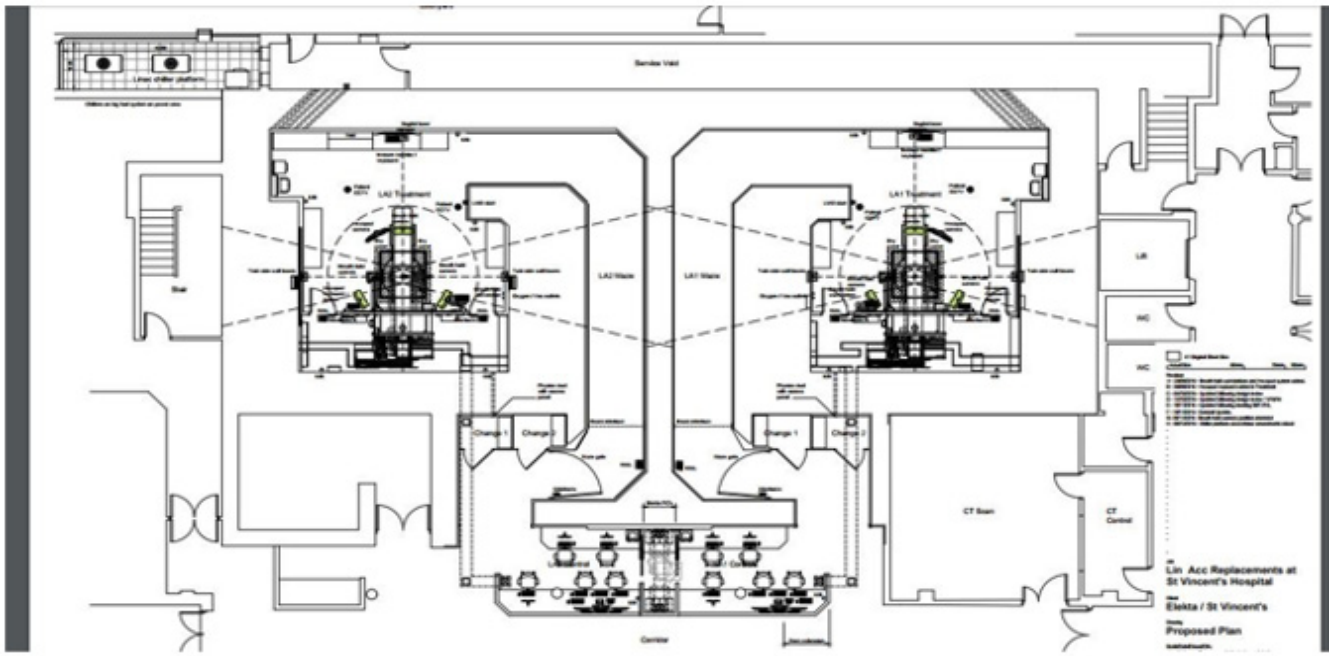

Figure K.2: Bunker plan of St. Vincent's Private Hospital Radiotherapy bunkers.